Genome-wide analysis of lncRNAs and mRNAs expression during the differentiation of abdominal preadipocytes in chicken

Tao Zhang[1], Xiangqian Zhang[1], Kunpeng Han[1], Genxi Zhang[1], Jinyu Wang[1,*], Kaizhou Xie[1]and Qian Xue[1]

[1] College of Animal Science and Technology, Yangzhou University, Yangzhou, Jiangsu, China, 225009.

The Sequencing data were submitted to the sequence Read Archive (Accession Number SRR3985377) in NCBI.

Running title: LncRNAs analysis of preadipocytes

Keywords: Preadipocytes differentiation; RNA-seq; Stage-specific module; Chicken

Corresponding author: Jingyu Wang

Mailing address: East Wenhui Road 48, Yangzhou city, Jiangsu province, China.

Phone number: +86-0514-87979075

Email: jywang@yzu.edu.cn

Abstract: lncRNAs regulate metabolic tissue development and function, including adipogenesis. However, little is known about the function and profile of lncRNAs in preadipocytes differentiation of chicken. Here, we identified lncRNAs in preadipocytes of different differentiation stages by RNA-sequencing using Jinghai Yellow chicken. A total of 1,300,074,528 clean reads and 27,023 lncRNAs were obtained from twenty samples. 3095 genes (1,336 lncRNAs and 1,759 mRNAs) were differentially expressed among different stages, of which the number of DEGs decreased with the differentiation, demonstrating that the early stage might be most important for chicken preadipocytes differentiation. Furthermore, 3,095 DEGs were clustered into 8 clusters with their expression patterns by K-means clustering. We identified six stage-specific modules related to A0, A2 and A6 stages using weighted co-expression network analysis. Many well-known/novel pathways associated with preadipocytes differentiation were found. We also identified highly connected genes in each module and visualized them by cytoscape. Many well-known genes related to preadipocytes differentiation were found such as *IGFBP2* and *JUN*. Yet, the majority of high connected genes were unknown in chicken preadipocytes. This study provides a valuable resource for chicken lncRNA study and contributes to batter understanding the biology of preadipocytes differentiation in chicken.

1. Introduction

The abdominal fat is an important carcass trait of broiler. The production performance of broiler has been significantly improved after decades of breeding and selection. However, the overemphasis on selection of broilers for rapid growth rate leads to excessive fat accumulation, especially for Chinese local chicken breeds. The excessive fat is often disposed as waste. Furthermore, excess fat deposition results in

65 reduction of feed conversion ratio, carcass yield, laying rate, fertility rate and hatching
66 rate. Lower abdominal fat therefore has become one of the breeding goals of broiler.
67 Adipose tissue is a complex, essential, and highly active metabolic and endocrine
68 organ(Kershaw and Flier, 2004). The growth of adipose tissue is primarily due to the
69 increase in adipocyte cell number (hyperplasia) and the enlargement of adipocytes
70 (hypertrophy). As is well known that adipocytes are derived from pluripotent
71 mesenchymal stem cells (MSCs) in adipogenesis process(Ding et al., 2015). The MSC
72 have ability to develop into adipoblasts, which then will develop into preadipocytes that
73 could store lipid. The preadipocytes can finally differentiate into adipocytes under
74 particular conditions(Leclercq, 1984). The cell number in mature adipose tissue is
75 thought to reflect the proliferation of preadipocytes and their subsequent differentiation
76 into mature adipocytes(Matsubara et al., 2013).
77 The adipogenesis process is controlled by a complex process that regulated by
78 various transcriptional events. In mammals, the differentiation of preadipocytes is well
79 studied, especially in human and mouse. Previous studies have identified that
80 peroxisome proliferator-activated receptor γ (*PPARγ*) and CCAAT/enhancer binding
81 proteins (*C/EBPs*) are key genes regulating adipocytes differentiation(MacDougald
82 and Lane, 1995; Morrison and Farmer, 2000). Matsubara et al. reported that PPARγ is
83 also a key regulator of preadipocyte differentiation(Matsubara et al., 2005). Rencent
84 studies in mammals have demonstrated functions of some new transcription factors in
85 adipogenesis, such as transcriptional factor of zinc finger protein 423 (*Zfp423*)(Gupta
86 et al., 2010), Krüppel-like transcription factors (KLFs) (*FGF10*)(Banerjee et al., 2003;
87 Kaczynski et al., 2003; Mori et al., 2005) and Fibroblast growth factor 10(Sakaue et al.,
88 2002; Yamasaki et al., 1999).

In chicken, several genes including *KLF2*(Zhang et al., 2014a), *KLF3*(Zhang et al., 2014b) and *FATP1*(Qi et al., 2013) are identified as regulator in chicken adipogenesis and preadipocytes differentiation. However, little is known about the details of how adipogenesis is regulated. Recently, several studies try to investigate the regulation mechanism of chicken adipogenesis by genome-wide analysis of mRNA(Ji et al., 2012; Regassa and Kim, 2015) and microRNA(Wang et al., 2015). In the present study, lncRNA and mRNA profiling of preadipocytes during differentiation were analyzed using RNA sequencing. Our study focused on characterizing the features of lncRNA and identifying differentially expressed lncRNAs and mRNAs between different differentiation stages of preadipocytes. The functions of differentially expressed genes were annotated and the pathways involved were enriched. Our study provides a valuable resource for chicken lncRNA study and contributes to batter understanding the biology of preadipocytes differentiation.

2 Materials and mathods

2.1 Primary culture of chicken preadipocytes from abdominal adipose tissue

Chicken preadipocytes from abdominal adipose tissue were cultured according to the method described by Shang(Shang et al., 2014), with some modifications. Abdominal adipose tissue was collected from 14-day-old Jinghai yellow chicken under sterile condition. Adipose tissue was washed by PBS supplemented with penicillin (100 units/ml) and streptomycin (100 μg/ml). The washed tissue was cut to 1 ㎜ 3 by surgical scissors and then digested using 2 mg/ml collagenase type I (Sangon Biotech) with shaking for 65 min at 37 ◦C. The digested cell suspension was filtrated using 200 and 500 mesh screens and centrifuged at 300g for 10min (22 ◦C) to separate the stromal-vascular fractions from undigested tissue debris and mature adipocytes.

Stromal-vascular cells were plated to 50mm culture palte at a density of 1×105 cells/ml and cultured with DMEM/F12 (Dulbecco's modified Eagle's medium/Ham's nutrient mixture F-12) basic medium (10% (v/v) FBS, 100 units/ml penicillin and 100 μg/ml streptomycin) in a humidified atmosphere with 5% (v/v) CO2 at 37 ◦C until reaching 90% confluence.

2.2 Induction of abdominal preadipocytes

Following 90%cell confluence, the basic medium was removed and replaced with differentiation medium (0.25 μM dexamethasone (Takara), 10 μg/ml insulin (Takara) and 0.5 mM IBMX (Takara) for 48 hours. The differentiation medium was replaced with maintenance medium (10 μg/ml insulin (Takara)) and incubated for 48 hours. The detailed procedure for induction of abdominal preadipocytes was described in Figure 1. Cells were collected after induced for 0h, 48h, 96h and 144h. Each point included 3 biological replicates (n=3).

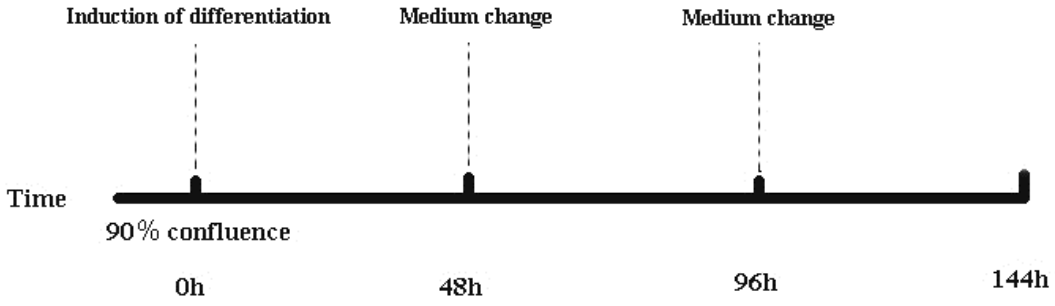

Figure 1. Induction differentiation procedure of abdominal preadipocytes. The basic medium consisted of DMEM/F12 and 10% FBS. Induction differentiation medium consisted of basic medium, insulin, dexamethasone and IBMX. Maintenance medium consisted of basic medium and insulin. Induction differentiation medium was replaced with maintenance medium at 48h, while maintenance medium was replaced with basic medium at 96h.

2.3 RNA extraction, library construction and sequencing

A total of 12 cell samples were successfully collected. Total RNA was extracted using Trizol reagent (Invitrogen). The integrity, concentration and purity of total RNA were checked via Nanodrop, Qubit 2.0 and Aglient 2100. RNA samples with a RIN value greater than 8.0 and an OD 260/280 ratio greater than 1.9 were selected for deep sequencing. The rRNA was removed and mRNA was enriched using magnetic bead with Oligo (dT) and then randomly fragmented by Fragmentation Buffer. The mRNA was used as template to synthesize the first-strand cDNA using 1st Strand Enzyme Mix (Enzyme). The second-strand cDNA was synthesized using 2nd Strand Marking Buffer and 2nd Strand/End Repair Enzyme Mix (Enzyme). The products were purified by VAHTS^{TM} DNA Clean Beads and then the end of double strand was repaired and A-tailed. An adapter was jointed to A-tailed products using ligation mix. Suitable sized fragments were selected using VAHTS^{TM} DNA Clean Beads to construct the cDNA library by PCR. The RNA sequencing was performed using Illumina HiSeq2500.

2.4 Quality control

The raw data was performed to quality control using FastQC (http://www.bioinformatics.babraham.ac.uk/projects/fastqc/). The base composition and quality distribution of reads and the GC and AT base content were analyzed, which could reflect the quality of raw data in whole. Clean Data was obtained by removing reads containing adapter, reads containing over 10 % of ploy-N, and low-quality reads (>50 % of bases whose Q scores were ≤10 %) from the raw data.

2.5 Sequencing data analysis and transcriptome assembling

Clean Data was mapped to the *Gallus gallus* reference genome (gal4) by Tophat(Trapnell et al., 2012) program using the following parameters:

157 --segment-length 25 –segment-mismatches 2. The remaining parameters were set as
158 default. The uniformity, insert length and saturation of sequencing data were analyzed
159 based on the alignment results. The transcripts were assembled using
160 cufflinks(Trapnell et al., 2012) program based on RABT Assembling strategies.

161 *2.6 lncRNA prediction*

162 Based on the assembling results, transcripts with RPKM=0 were wiped off. The
163 filter criteria of lncRNA were: 1) removed transcripts shorter than 200nt; 2) removed
164 transcripts with a ORF that was longer than 300nt; 3) removed transcripts containing
165 specific domain; 4) transcripts that were similar to known protein; 5) transcripts that
166 were predicted to coding by CPC.

167 *2.7 lncRNA targets prediction and annotation*

168 lncRNA functioned by acting on protein coding gene via *cis*-acting element and
169 trans-acting factor. In the present study, lncRNA targets were predicted based on *cis*
170 function prediction. The closest coding genes to lncRNAs in 10K of upstream and
171 downstream were screened and their associations with lncRNA were analyzed using
172 Bedtools program(Quinlan and Hall, 2010). Then the target genes were conducted to
173 functional enrichment analysis using the DAVID database(Huang da et al., 2009).

174 *2.8 Quantitation of gene expression*

175 Cuffdiff(Trapnell et al., 2013) was used to calculate reads per kb for a million reads
176 (RKPM) of both mRNA and lncRNA in each sample. For biological replicates,
177 transcripts or genes with a $p<0.05$ and foldchange≥2 were defined as differential
178 expressed genes or lncRNAs between two groups(Ren et al., 2016).

179 *2.9 Co-expression network analysis*

The co-expression network was contructed by Weighted Gene Co-expression Network Analysis (WGCNA) package(Langfelder and Horvath, 2008) in R environment with the 3,095 differentially expressed genes. Module was detected by dynamic tree cutting method. Then the stage-specific modules were identified based on the correlation between eigengene and traits. Module with a *P*-Value <0.05 was defined as significant. We identified the central and highly connected genes by visualizing the top 200 connections of the top 150 genes for each stage-specific module.

2.10 Gene ontology and Kyoto Encyclopedia of Genes and Genomes analysis

Functional annotation enrichment analysis for Gene Ontology (GO) and Kyoto Encyclopedia of Genes and Genomes (KEGG) were conducted by DAVID database(Huang da et al., 2009). Go terms and pathways with *P* value less than 0.05 were considered as significantly enriched.

2.11 Validation of gene and lncRNA expression by qRT-PCR

Primers were designed using the Primer-BLAST in NCBI (http://www.ncbi.nlm.nih.gov/tools/primer-blast/) (Table 1). The first cDNA strand was synthesized using PrimeScript™ RT Master Mix (Perfect Real Time) kit (Takara, JPN) according to the user manual. β-actin was used as housekeeping gene. Expression of lncRNA and mRNA were quantified using SYBR® Premix Ex Taq™ II kit (Takara, JPN). The 20 μL PCR reaction included 10 μL SYBR Premix Ex Taq II (TaKaRa, Dalian,China), 0.4 μL (10 p moL / μL) specific forward primer, 0.4μL (10 p moL /μL) reverse primer, 0.4 μL ROX reference dye, 2 μL (10 ng/μL) diluted cDNA and 6.8 μL RNase free water. Cycling parameters were 95 ℃ for 30 s, followed by 40 cycles of 95 ℃ for 5 sec and 60 ℃ for 34 sec. Melting curve analyses were performed following

amplifications. The ABI 7500 software was used to detect the fluorescent signals. Quantification of selected gene expression was performed using the comparative threshold cycle ($2^{-\Delta\Delta CT}$) method.

Table 1 Primers of genes for qRT-PCR

GeneID	Primer sequence	Accession nember	Product length
ACTR6	F: CACGTCAGCGTCATTCCCAA R: GCCGGAGGGGTCTTTGATTT	NM_204637.1	99
CHD6	F: ACACACAGGGCAATCCTCTC R: CCTGTTCTTCAAGCGATGCG	XM_015296251.1	146
LLGL1	F: CTCCAGCAAGGAGGCCAAC R: AGGTGTCGGCGAAGTAAAGG	XM_015294418.1	146
NEURL1B	F: ACAGCAGCTTCCAAGACACA R: GTTGGGCAGGCTGTAGTAGG	XM_015293830.1	71
XLOC_045161	F: TCAGAGGCCAATACTCCGAAA R: AACACCCTGGAAAGAGCGTG	TCONS_00063548[a]	102
XLOC_070302	F: ATGTGGGTGAGTTGTGTCGG R: TGTGATCCAAGGCATCGCTC	TCONS_00097398	87
XLOC_068731	F: GGCTTATCCCTCAAGCCCC R: ATGGCCGGAAATGATTCGCA	TCONS_00095558	101
XLOC_022661	F: CATGCTCTGGTGCTGGAATC R: CTGCTATCCGGAAGCGTGAA	TCONS_00031800	107

a: the sequences of lncRNAs can be found in Table S1.

The Sequencing data of our study were submitted to the sequence Read Archive (Accession Number SRR3985377) in NCBI. Supplemental materials include ten files. Table S1 contains the names and sequences of all the candidate lncRNAs. Table S2 contains all the differentially expressed lncRNAs and mRNAs. The common differentially expressed lncRNAs and mRNAs among three comparisons (A0 vs A2, A2 vs A4, A4 vs A6) are included in Table S3. Table S4, Table S5 and Table S6 are the GO and pathway analysis of target genes of lncRNAs, DEGs of different stages and co-expressed mRNAs with lncRNAs, respectively. Table S7, Table S8 and Table

S9 are the annotation of genes in A0, A2 and A6 stage-specific modules, respectively. The validation of RNA-seq using qRT-PCR is included in Table S10. Figure S1 and Figure S2 are GO analysis of DEGs of different stages and visualization of the co-expression network of all DEGs.

3. Results

3.1 Sequencing results and quality control

A total of 1,394,219,096 raw reads were produced from 12 cDNA libraries. After quality control, 1,300,074,582 clean reads (195.02 Gb) were obtained. The percentage of clean reads among raw reads in each library ranged from 91.41% to 94.73 %. The percentage of reads with a Phred quality value greater than 30 among clean reads ranged from 92.95% to 94.30%. The average GC content of clean reads in 12 samples was 52.51%. Subsequently, the clean reads were aligned with the chicken reference genome (http://hgdownload.soe.ucsc.edu/goldenPath/galGal4/bigZips/galGal4.fa.gz). The mapped rate of 12 samples ranged from 79.40% to 84.30%. Among these mapped reads, 66.17%-70.07% of reads were mapped to CDS regions, 5.34%-8.18% to intron regions, 14.49%-16.08% to intergenic regions, and 8.83%-11.00% to UTR regions (Table 2). High Pearson correlation coefficients were found among biological replicates of the same differentiation stage, which indicated the reproducibility of sample preparation (Figure 5A).

Table 1 Statistics of clean reads in preadipocytes of chicken

	A0-1	A0-2	A0-3	A2-1	A2-2	A2-3	A4-1	A4-2	A4-3	A6-1	A6-2	A6-3
Total clean reads	114225220	138217716	110196390	124574594	104305988	117527324	103271936	118853588	116411784	97058458	807271 60	47404424
Base numbe r(G)	17.13	20.73	16.53	18.69	15.65	17.63	15.49	17.83	17.46	14.56	12.11	11.21

Q30 reads (%)	94.13	94.28	94.30	93.86	93.35	93.90	92.81	93.04	93.15	93.18	93.20	92.95
Mapped reads	950861 76	114733 972	895112 92	105009 893	869954 36	989637 34	869849 09	943193 05	929220 64	81432 206	660102 94	61915 627
CDS(%)	68.53	69.93	70.07	69.32	68.73	68.55	66.91	69.80	67.62	66.67	68.50	66.17
Intron(%)	5.86	5.34	5.85	6.36	6.82	7.09	7.32	6.31	7.38	8.18	6..77	8.28
Intergenic (%)	14.60	14.50	14.83	14.49	14.65	14.59	14.93	14.90	15.68	15.11	15.90	16.08
UTR(%)	11.00	10.22	9.25	9.83	9.80	9.77	10.84	9.00	9.33	10.03	8.83	9.47

3.2 Identification of lncRNAs in abdominal preadipocytes

We used five tools, namely NONCODE, TransDecoder, Pfam, BlastX and CPC, to remove potential coding and short (length<200nt) transcripts. Finally, 27,023lncRNAs were obtained (Table S1). The length and exon number of lncRNAs were analyzed. We found that lncRNAs were shorter in length and fewer in exon number than protein coding genes in abdominal preadipocytes (Figure 2).

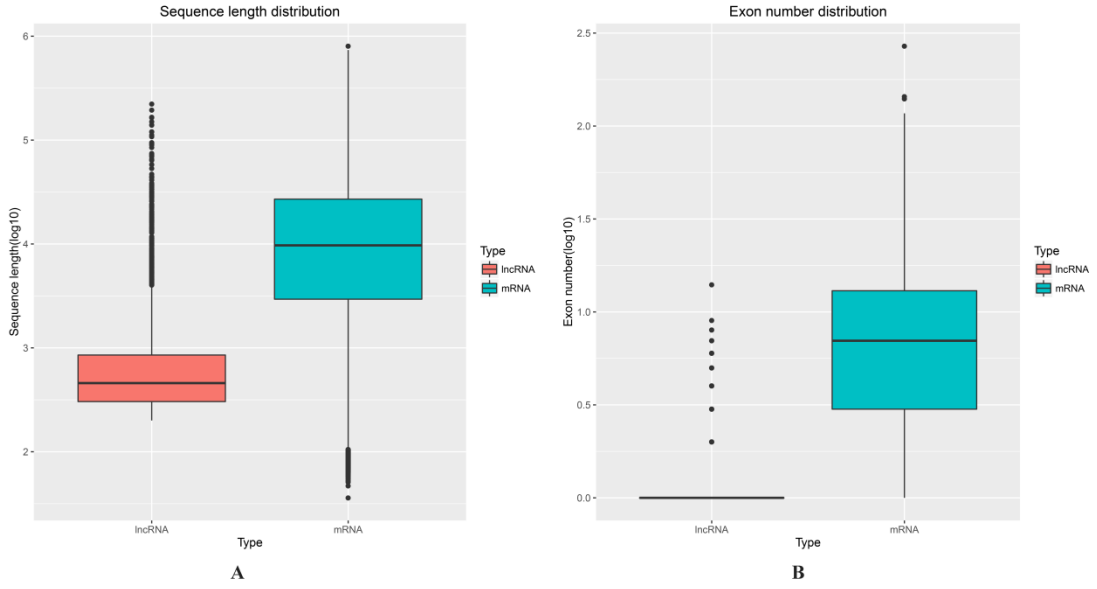

Figure 2. Length and exon number of lncRNAs and mRNAs. (A) Length distributionog mRNAs and lncRNAs. (B) Exon number distribution of mRNAs and lncRNAs.

3.3 Differentially expressed lncRNAs and mRNA during abdominal fat preadipocytes differentiation

Given a *P* value < 0.05 and Fold change≥2, 1,336 differentially expressed lncRNAs and 1,759 differentially expressed mRNAs were obtained by pairwise comparison (A0 vs A2; A0 vs A4; A0 vs A6; A2 vs A4; A2 vs A6 and A4 vs A6) of samples collected from preadipocytes at day 0, 2, 4 and 6 of differentiation (Figure 3A, 3B) (Table S2). No common gene was identified among 6 comparisons. 936 differentially expressed lncRNAs and 1,280 differentially expressed mRNA were obtained by pairwise comparison (A0 vs A2; A2 vs A4; A4 vs A6) of the same samples. As shown in figure3C, D, 30 differentially genes (DEGs) were common among three comparisons (7 lncRNAs and 23 mRNAs) (Table S3). We counted the DEGs number of three comparisons (A0 vs A2, A2 vs A4 and A4 vs A6) (Figure 3E, F). The results showed that the number of differentially expressed mRNAs and lncRNAs decreased with the differentiation of preadipocytes.

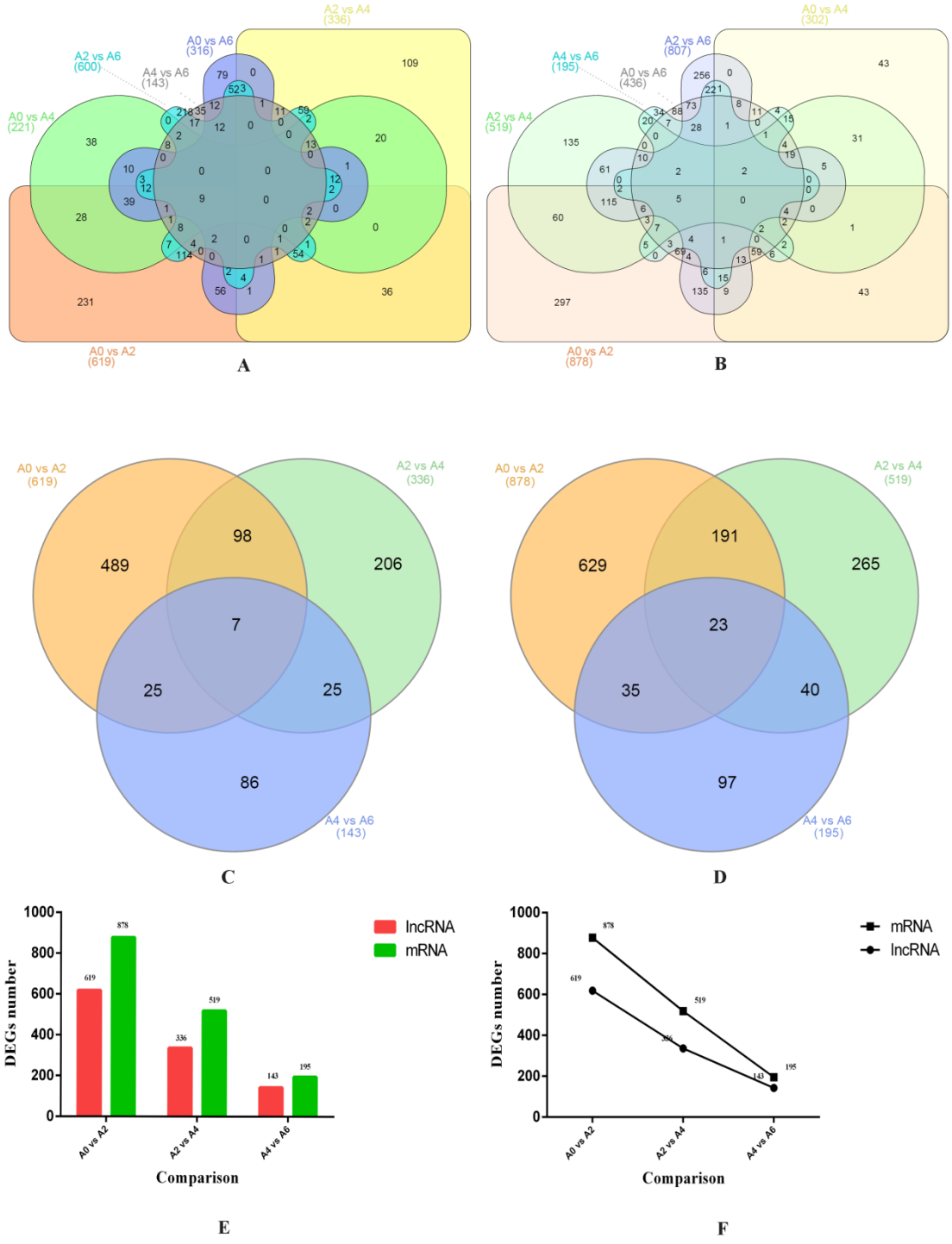

Figure 3. Venn diagram of DEGs at different stages. (A) Venn diagram of common LncRNAs in six comparison (A0 vs A2, A0 vs A4, A0 vs A6, A2 vs A4, A2 vs A6 and A4 vs A6). (B) Venn diagram of common mRNAs in six comparison (A0 vs A2, A0 vs A4, A0 vs A6, A2 vs A4, A2 vs A6 and A4 vs

A6). (C) Venn diagram of common LncRNAs in three comparisons (A0 vs A2, A2 vs A4 and A4 vs A6). (D) Venn diagram of common mRNAs in three comparisons (A0 vs A2, A2 vs A4 and A4 vs A6). (E) Histogram of DEGs number in three comparisons. (F) Line chart of DEGs number in three comparisons.

We performed K-means clustering of all DEGs using the euclidean distance method associated with complete linkage (Figure 4). Eight clusters were plotted with expression patterns (Table S4). The K1 cluster included 392 genes which showed up-regulated at day two of differentiation and then down-regulated at day 4 and 6 of differentiation. The 49 genes in K2 were up-regulated across the whole induction process. The expressions of 159 genes in K3 were slightly down-regulated at A4 and A6 stage compared to A0 and A2 stage. K5 cluster included most of the DEGs which expressed smoothly across four stages proceeded. The genes in K5 and K5 clusters had opposite expression pattern. The genes in K5 were significantly down-regulated at A2, A4 and A6 stages compared to the first stage, whereas, the genes in K6 were significantly up-regulated at A2, A4 and A6 stages compared to the first stage. The expression level of genes in K7 remained stable at first two stages and then was up-regulated at last two stages.

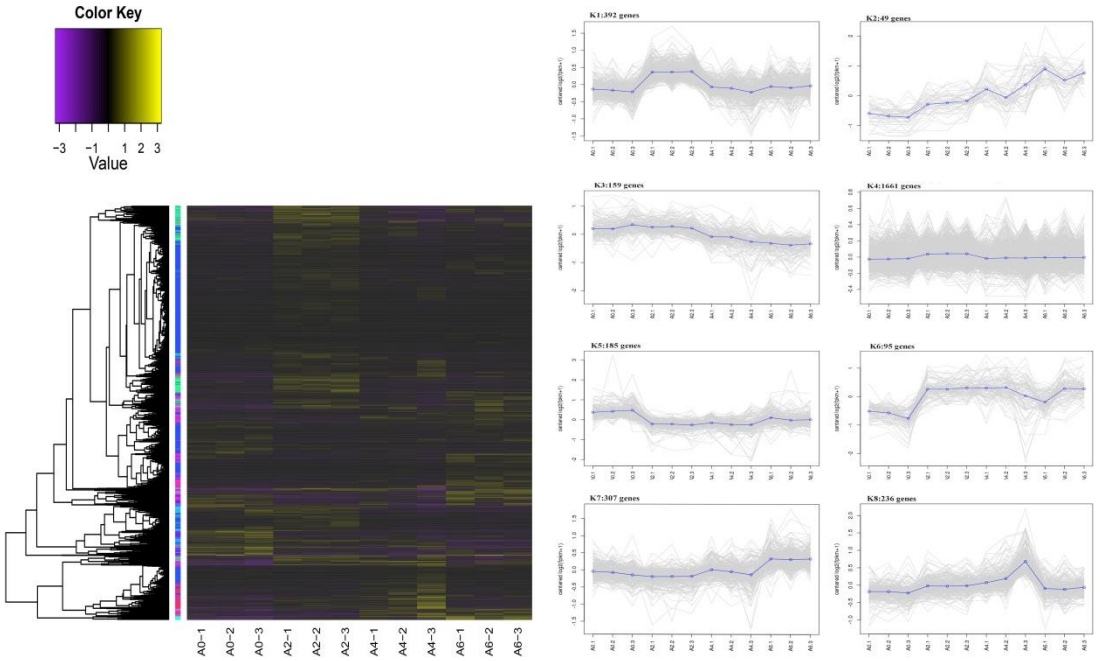

Figure 4. Clustering of all DEGs (lncRNAs and mRNAs). (A) The heat map shows the K-means clustering of transformaed expression values for lncRNAs and mRNAs. Yellow represents higher expression and purple represents lower expression. (B) expression patterns of genes in eight clusters corresponding to the heat map.

3.4 Functional prediction of lncRNAs and mRNAs in preadipocytes samples

We selected coding genes 10K upstream and downstream of lncRNAs as the *cis* target genes(Ren et al., 2016; Wang et al., 2016). Finally, 4915 target genes were identified. To predict the function of lncRNAs in preadipocytes of chicken, we performed GO and KEGG analysis with the *cis* target genes (Table S4). A total of 1746, 1544 and 2174 genes were assigned to biological process, cellular component and molecular function GO categories, respectively. In the biological process category, 27 terms such as cellular process, system development and anatomical structure development were significantly enriched. In cellular component category, the top three

terms were intracellular, intracellular membrane-bounded organelle and membrane-bounded organelle, while in molecular function category, protein binding and binding protein serine/threonine kinase activity were the most abundant terms. The KEGG enrichment showed that 971 out of 4915 genes were significantly enriched in 9 pathways including Wnt signaling pathway, MAPK signaling pathway and Vascular smooth muscle contraction pathway.

To gain insight into the similarities and differences in differentiation of three stages , the differential expressed mRNAs of three comparisons (A0 vs A2, A2 vs A4, A4 vs A6) were conducted to GO and KEGG pathway analysis (Table S5). In the biological process category, most of the genes were involved in processes associated with cellular regulation and metabolism, such as cellular process, cellular macromolecule metabolic process and cellular metabolic process. The top three GO terms were cellular process, metabolic process and primary metabolic process at A0-A2 and A4-A6 stages, while they were biological regulation, regulation of biological process and regulation of cellular process at A2-A4 stage (Figure S1). KEGG analysis showed that, in the top fifteen pathways, five pathways were common among three stages. They were Cell cycle, Cytokine-cytokine receptor interaction, Jak-STAT signaling pathway, Oocyte meiosis and Ubiquitin mediated proteolysis pathways. Furthermore, 5, 4 and 5 stage-specific pathways were identified for three differentiation stages. Stage-specific pathways with the highest number of DEGs for A0-A2, A2-A4 and A4-A6 stages were Oxidative phosphorylation, Regulation of actin cytoskeleton and Glycosphingolipid biosynthesis, respectively.

3.5 Co-expression network and module construction

In our study, WGCNA R software package was used to perform the co-expression network analysis. lncRNAs exerted its biological functions by regulating target

mRNAs. The co-expression network could help us to predict target mRNAs of lncRNAs, which shared common expression patterns. To gain insight in the functions of differential expressed lncRNAs, we constructed co-expression network with 1336 and 1759 differential expressed lncRNAs and mRNAs (Figure S2). The node and edge files respond to gene expression profiles and pairwise correlations between gene expressions, respectively. 106 mRNAs were identified to have common expression patterns with 176 lncRNAs, which might be target genes of lncRNAs (Table S6). The 106 mRNAs were conducted to GO and KEGG analysis to predict the functions of lncRNAs. GO analysis showed that signal transduction, regulation of biological process and system development were the top three terms in biological process category. In molecular function category, insulin-like growth factor binding, nucleoside-triphosphatase activity and pyrophosphatase activity terms were significantly enriched while in cellular component, trans-Golgi network transport vesicle was significantly enriched. No significant pathway was enriched. However, several well-known pathways involved in differentiation of preadipocytes were identified, including ErbB, MAPK, Insulin and Jak-STAT signaling pathway.

Weighted gene co-expression network analysis can be used for finding clusters (modules) of highly correlated genes, for summarizing such clusters using the module eigengene or an intramodular hub gene, for relating modules to one another and to external sample traits(Langfelder and Horvath, 2008). In our study, 3,095 DEGs were used to identify groups of co-expressed genes, termed “modules”. Each module is assigned a unique color label underneath the cluster tree(de Jong et al., 2012). Ten modules were identified in size ranging from 99 genes in the purple module to 524 in the blue module (Figure 5B). The co-expression modules could not exist independent, instead, they formed a meta-network. To explore and identify the correlations among

355 modules, the modules were conducted to clustering analysis based on their eigengenes.
356 The results showed that ten modules were classified into 4 groups: the first was
357 turquoise module; the second included magenta, brown and pink modules; the third
358 included purple and red modules; the fourth included blue, black, green and yellow
359 modules (Figure 5C). Modules classified into same group might have same or similar
360 functions and regulation mechanisms.

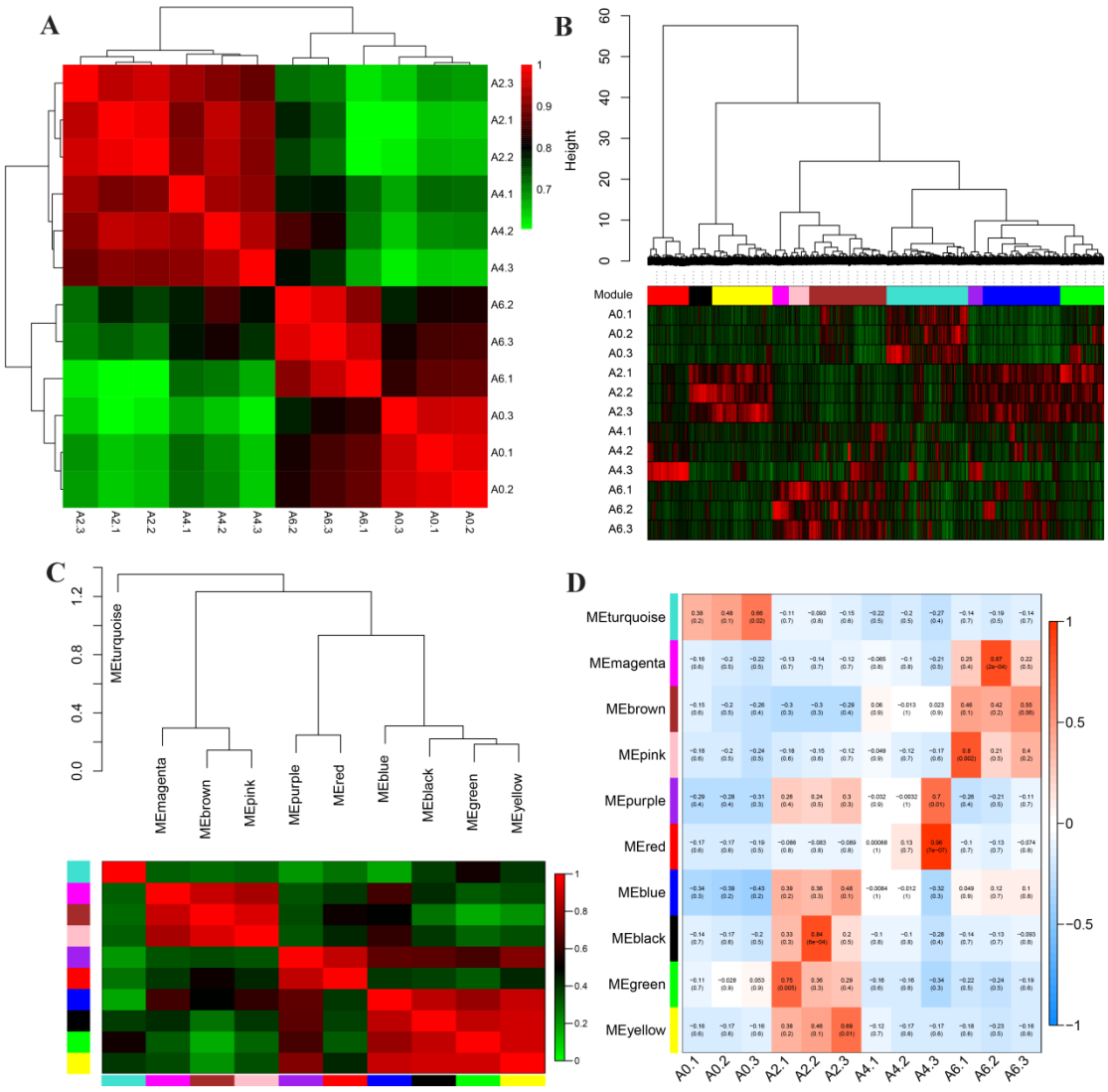

361

362

363 Figure 5 Visualization of co-expression network construction. (A) Heatmap of
364 duplicate samples of chicken abdominal preadipocytes differentiation. The

color, ranging from green through dark to red, represents pearson correlation coefficients ranging from 0.6 to 1, indicating low to high correlations. All samples in the same differentiation stage are highly correlated in pearson coefficients indicating the reproducibility of the samples. (B) Hierarchical cluster tree (average linkage, dissTOM) of the 3095 genes. The color bands provide a simple visual comparison of module assignments (branch cuttings) based on the dynamic hybrid branch cutting method. (C) Clustering of modules based on eigengenes. The color, ranging from green through dark to red, represents pearson correlation coefficients ranging from 0 to 1, indicating low to high correlations. (D) Heatmap of correlations between module and differentiation stage. The color, ranging from blue through white to red, indicates low to high correlations.

3.6 Identification and visualization of stage-specific module

To explore stage-specific modules during chicken abdominal preadipocytes differentiation development, we calculated the *gene significance* (GS) and *module membership* (MM) of all genes within a module. GS was defined as (the absolute value of) the correlation between the gene and the differentiation stage. MM was defined as the correlation of the module eigengene and the gene expression profile. We identified six stage-specific modules (FDR $P<0.05$) (Figure 6), in which the black, blue, green and yellow modules were positively correlated with A2 stage (Figure 6A, B, D, F) while the turquoise and brown modules were positively correlated with A0 and A6 stages (Fig 6C, E), respectively. It meant that the genes in modules above were predominantly up-expressed at day 2, day 0 and 6 of differentiation. Furthermore, the blue module also was negatively correlated with A0 stage, meaning that the genes in blue module were predominantly down-expressed at day 0 of differentiation. We also

found that the magenta, pink and purple modules, though not significant (FDR P>0.05), might play important role in preadipocytes differentiation when it comes to their expression pattern (Figure 5B, D). Genes in magenta and pink modules expressed in low level before day 4 of differentiation and then achieved a relatively high expression level at day 6 of expression. Similarly, the genes in purple module expressed low at day 0, increased their expression level at day 2 and then decreased their expression level at day 4 and 6 of differentiation.

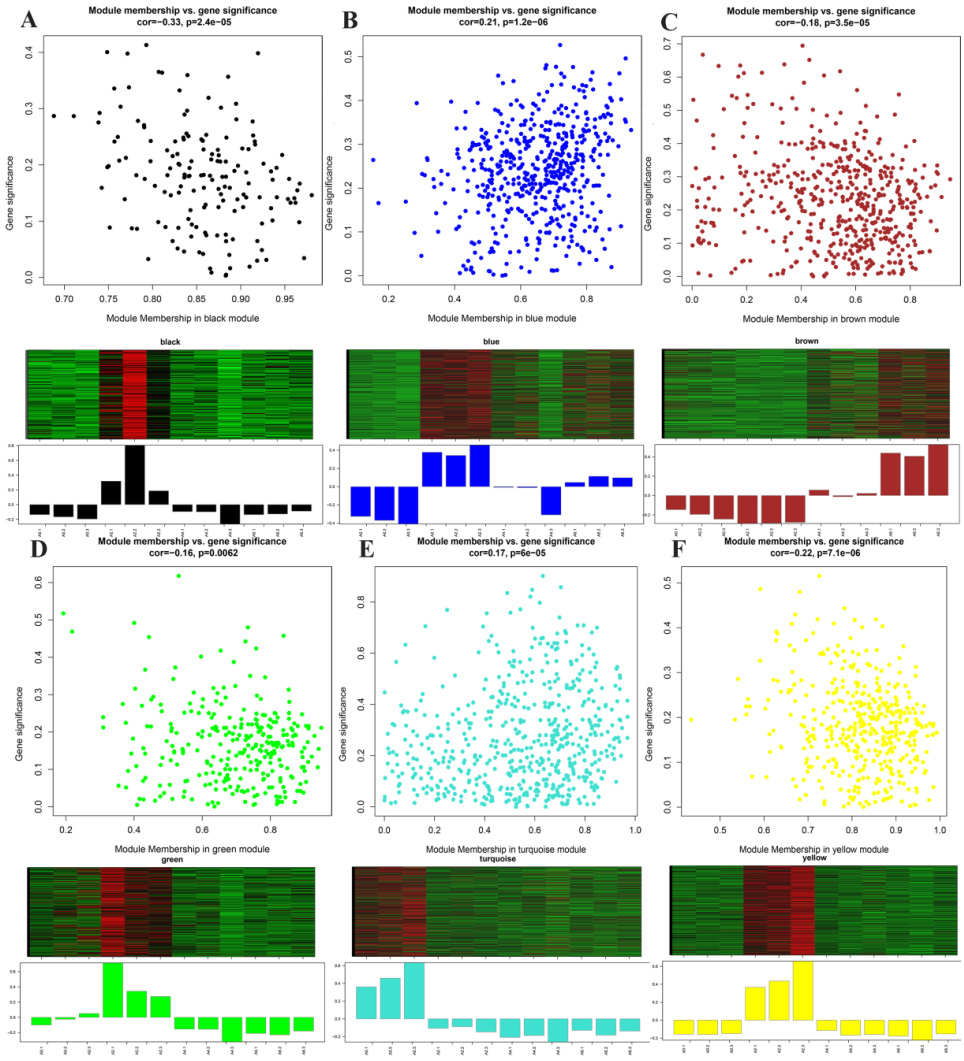

Figure 6. visualization of GS vs MM and gene expression level of significant modules. Scatterplot represents the GS and MM of each module, which exhibits a significant correlation between GS and MM (P<0.05), implying that

module tend to be associated with differentiation stage. Clustering heatmap and barplot represent gene expression level of each module. In the heatmap, the color range from green through dark to red indicates low to high expression level.

3.7 identification of central and high connected genes

In order to identify genes that are central and highly connected in the stage-specific modules, we analyzed top 200 connections of the top 150 highly connected genes for each stage-specific module and visualized them using Cytoscape (Figure 7). Five common genes (Three lncRNAs and two mRNAs) were identified among four highly correlated modules of black, blue, green and yellow. It suggested that XLOC_068731, XLOC_022661, chromodomain helicase DNA binding protein 6 (*CHD6*), lethal giant larvae homolog 1 (*LLGL1*) and neuralized E3 ubiquitin protein ligase 1B (*NEURL1B*) might play important roles in differentiation of A2 stage. In the brown module, Kelch like family member 38 (*KLHL38*) and XLOC_045161 were the highest connected mRNA and lncRNA, indicating their potential key roles in regulation of preadipocytes differentiation at A6 stage. ARP6 actin-related protein 6 homolog (*ACTR6*) and XLOC_070302, with the most connection, were found to be important factors in A0 stage of differentiation.

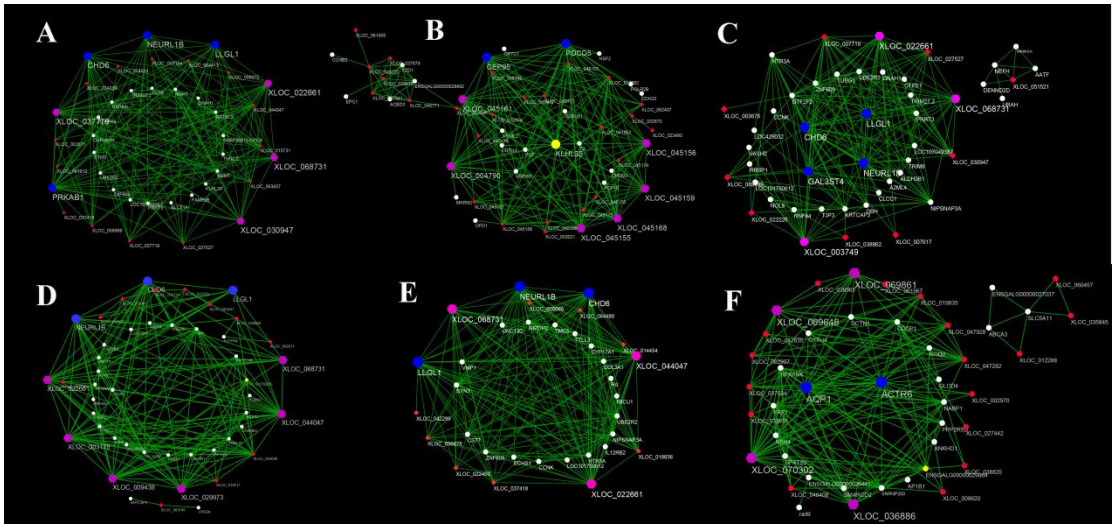

Figure 7. visualization of connections of genes in modules. A, B, C, D, E and F represent the visualization of connections of genes in black, brown, green, yellow, blue and turquoise modules. Red-colored nodes represent mRNAs. White-colored nodes represent lncRNAs. Pink-colored and blue-colored nodes indicate common and highly connected lncRNAs and mRNAs, suggesting their central role in the network.

3.8 GO and pathway analysis of genes in stage-specific modules

GO analysis reveals the functions of genes in stage-specific modules and pathway analysis reveals essential signaling and metabolic networks in preadipocytes differentiation. The enriched GO terms of biological process and pathways were showed in Table S7, S8 and S9. For GO analysis, RNA metabolic process, regulation of localization and cellular metabolic process were significantly enriched at A0 stage, generation of precursor metabolites and energy, electron transport chain and energy derivation by oxidation of organic compounds were highly enriched at A2 stage, while blastocyst development and cellular process were greatly enriched at A6 stage (P<0.05). In the pathway analysis, no significant pathway was identified at A0 and A6 stages. Oocyte meiosis, Lysosome and Galactose metabolism were the top three pathways at

438 A0 stage, while Biosynthesis of unsaturated fatty acids, Apoptosis and Propanoate
439 metabolism were top three pathways at A6 stage. When it came to A2 stage, Oxidative
440 phosphorylation was significantly enriched ($P<0.05$). Interestingly, three common
441 pathways for Oxidative phosphorylation, Lysosome and Propanoate metabolism were
442 found in different differentiation stages. Additionally, many well-known pathways
443 related to preadipocytes differentiation including ABC transporters, Jak-STAT, Wnt,
444 Insulin, Fatty acid metabolism and Fatty acid biosynthesis signaling pathways were
445 found.

446 *3.9 Validation of DEGs by qRT-PCR*

447 Quantitative real time PCR (qRT-PCR) was carried out to validate the central and
448 highly connected genes XLOC_045161, XLOC_070302, XLOC_068731,
449 XLOC_022661, *ACTR6*, *CHD6*, *LLGL1* and *NEURL1B*. We used the same 12 cell
450 samples as were used in the RNA-seq for qRT-PCR validation. The qRT-PCR results
451 for all the genes were tested statistically by the T-test method. The results showed that
452 the expression patterns of these 8 genes were in excellent agreement with the RNA-seq
453 results(Figure 8, Table S10).

454

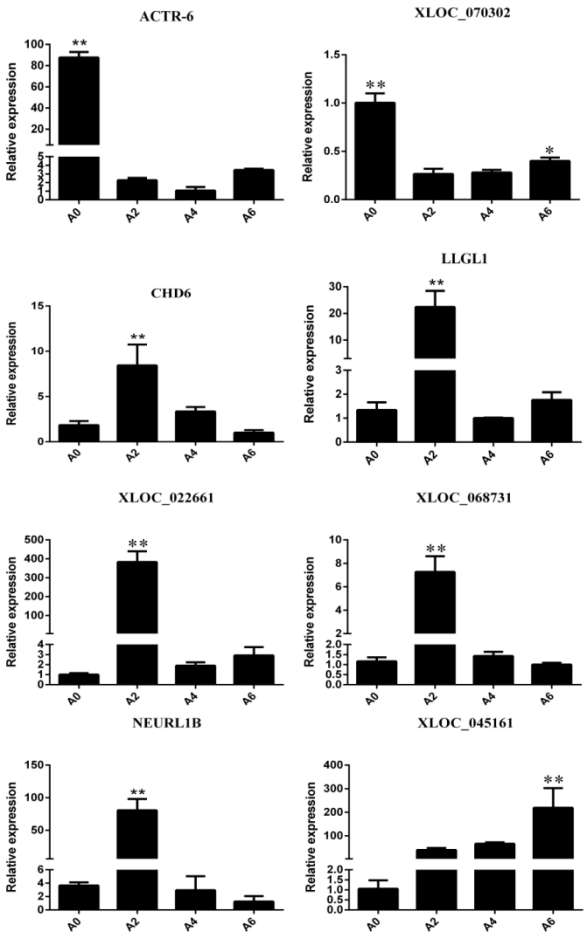

Figure 8. Validation of highly connected genes using qRT-PCR

4. Discussion

In the last 60 years, the selection of important economic traits has been the focus and significant genetic improvements have been gained(Dong et al., 2015). Genetic selection for enhanced growth rate in meat-type chickens (Gallus domesticus) is usually accompanied by excessive adiposity, which has negative impacts on both feed efficiency and carcass quality(Resnyk et al., 2015). The genetic improvement of abdominal fat by standard selection has been lower for two reasons: (1) intensity of selection has been lower because of the difficulty and cost to measure these phenotypes, and (2) genetic evaluations have been less accurate because evaluation of candidates is

467 based on information from relatives only(Demeure et al., 2013). Exploring the
468 molecular regulation mechanisms of fat deposition in broilers is helpful for optimal
469 breeding. Many studies have been carried out on gene expression of chicken abdominal
470 fat using genome-wide RNA sequence(Resnyk et al., 2013; Resnyk et al., 2015; Zhuo
471 et al., 2015).

472 Long non-coding RNA (lncRNA) is a kind of non-coding RNA longer than 200 nt,
473 which has attracted much attentions in the past several years. Studies show that
474 lncRNAs regulate metabolic tissue development and function, including adipogenesis,
475 hepatic lipid metabolism, islet function, and energy balance(Alvarez-Dominguez et al.,
476 2015; Chen et al., 2015; Luan et al., 2015; You et al., 2015; Zhao and Lin, 2015).
477 Despite the fact that many studies indicate the important role of lncRNA in different
478 tissues, little is known about the biological function of lncRNAs in chicken fat
479 deposition, especially in chicken preadipocytes differentiation. Our study was the first
480 to screen for lncRNAs and mRNAs regulating chicken preadipocytes differentiation by
481 sequencing and annotating the transcriptome of four preadipocyte differentiation stages.
482 After quality control, an average of 16.25 Gb clean reads were obtained per
483 preadipocyte sample. A total of 1,073,884,908 reads were successfully mapped to the
484 chicken reference genome assembly. As first study of lncRNAs in preadipocyte of
485 chicken, we identified 27,023 novel lncRNAs. Many studies have showed that
486 lncRNAs were fewer in exon number, shorter in length than mRNAs. Our results
487 indicated that the predicated lncRNAs were shorter in length and contain fewer exon
488 than mRNAs, which were in agreement with previous studies(Trapnell et al., 2010;
489 Wang et al., 2016).

490 To identify genes that associated with the differentiation of preadipocytes for
491 chicken, we compared the transcriptome-wide gene expression profiles between the

492 libraries of the four differentiation stages. 1,336 differentially expressed lncRNAs and
493 1,759 differentially expressed mRNAs were obtained by pairwise comparison. To
494 explore the stage which played crucial role in the preadipocytes differentiation, the
495 histogram and line chart of DEGs for different stages were plotted (Figure 3E, F). The
496 results showed that the number of differentially expressed lncRNAs and mRNAs
497 decreased with the differentiation of preadipocytes, which suggested that the early
498 stage might be most important for chicken preadipocytes differentiation. The
499 differential expressed mRNAs from three comparisons (A0 vs A2, A2 vs A4, A4 vs A6)
500 were performed to GO and KEGG analysis to explore the similarities and differences of
501 three stages. GO analysis showed that A0-A4 stage and A4-A6 stage were similar in
502 biological process while different from A2-A4 stage. KEGG results showed that among
503 the three comparisons, five pathways were common, in which the JAK-STAT signaling
504 pathway mediated the action of a variety of hormones that had profound effects on
505 adipocyte development and function. It suggested that JAK-STAT might play
506 important roles in the differentiation of chicken preadipocytes.

507 Dynamic changes of gene expression reflect an intrinsic mechanism of how an
508 organism responds to developmental and environmental signals. Genes with a similar
509 expression pattern are often hypothesized to have function dependence and might be
510 coregulated by some common regulatory factors(Ye et al., 2015). Genes with known
511 functions in a particular cluster can be a bait to point out a potential role of other
512 function-unknown genes, facilitating the prediction of gene functions. In our study,
513 3,095 DEGs were successfully clustered into eight clusters. We found several
514 interesting and important clusters associated with preadipocytes differentiation stage.
515 Genes in K 1 cluster showed significantly and specifically up-regulated at day two of
516 differentiation, indicating that they might greatly and specifically contribute to the

starting of the preadipocytes differentiation. Genes in K6 cluster were up-regulated at day 2, 4 and 6 compared to 0 day of differentiation, suggesting their roles in the entire differentiation process. K7 cluster consisted of 307 genes that were significant up-regulated at day 6 of differentiation, demonstrating that those genes might play important roles in the later stage of differentiation. Particular attention was paid to K2 cluster which included genes that underwent an overall trend of increase, suggesting their key roles over the entire differentiation process. Members from this cluster such as *GPR39* and *CHCHD4* had been reported to regulate the differentiation of preadipocytes(Dong et al., 2016).

To investigate the function of lncRNAs, we predicted the potential targets of lncRNAs in *cis* by searching for protein-coding genes 10 kb upstream and downstream of the lncRNAs, respectively. 4,915 potential target protein-coding genes that corresponded to 10,306 lncRNAs were found and performed to GO and pathway analysis. In the biological process category, 27 terms were significantly enriched, including cellular process, system development and anatomical structure development. Besides, we found that most of the 27 significant terms were related to regulation of gene expression such as regulation of cellular process, regulation of biological process and regulation of cell communication, clearly demonstrating the role of lncRNAs in the genome. Pathway analysis showed 971 genes were enriched in 131 KEGG pathways, in which 6 pathways were associated with preadipocytes differentiation such as Wnt signaling pathway, MAPK signaling pathway and Jak-STAT signaling pathway. These results suggested that lncRNAs act on its neighoring protein-coding genesin cis to regulate abdominal preadipocytes differentiation.

Studies has shown that genes and their protein products carry out cellular processes in the context of functional modules and are related to each other through a complex

542 network of interactions. Understanding an individual gene or protein's network
543 properties within such networks may prove to be as important as understanding its
544 function in isolation(Barabasi and Oltvai, 2004; Carlson et al., 2006; Hartwell et al.,
545 1999). Therefore, the primary emphasis in our study was on the constructing
546 co-expression network and detecting modules related to preadipocytes differentiation.
547 In our study, the integrated weighted gene co-expression network analysis (WGCNA)
548 was used to construct co-expression network and detect module with 3,095 DEGs in 12
549 samples(Fuller et al., 2007). Using WGCNA we identified ten modules, among which
550 six modules were stage-specific(Zhang and Horvath, 2005). It meant that those
551 modules included genes that were down expressed or over expressed in a particular
552 differentiation stage and can be used to represent the corresponding stage of
553 differentiation(Jiang et al., 2014). The black, blue, green and yellow modules were
554 correlated with stage of day two of differentiation (A2 stage), while the turquoise and
555 brown modules were correlated with day 0 (A0 stage) and day 6 (A6 stage) of
556 differentiation. Gene in one module suggested that they were involved in a common
557 network of biological processes and functions. To gain insight into the biological
558 processes and pathways involved in different stages of abdominal preadipocytes
559 differentiation, GO and pathway analysis were performed to genes in stage-specific
560 module. For A2 stage, given their high correlations (Figure 5C), the balck, blue, green
561 and yellow modules were merged in GO and pathway analysis. In the GO analysis,
562 RNA metabolic process, regulation of localization and cellular metabolic process were
563 significantly enriched at A0 stage, generation of precursor metabolites and energy,
564 electron transport chain and energy derivation by oxidation of organic compounds were
565 highly enriched at A2 stage, while blastocyst development and cellular process were
566 greatly enriched at A6 stage. Interestingly, we found that the functions of genes

567 migrated from RNA editing at A0 stage, to generation of precursor metabolites and
568 energy at A2 stage and finally to regulation of cell death and apoptosis at A6 stage. As
569 far as we know, quite a few pathways involved in preadipocytes differentiation have
570 been validated to date, including the PI3K/AKT cell signaling pathway(Dong et al.,
571 2016), LKB1-AMPK Pathway(Tung et al., 2016), Wnt/β-catenin signaling pathway(Lu
572 et al., 2016; Mai et al., 2014; Zhang et al., 2014c), TGF-β pathway(Park et al., 2014),
573 Bmp/Smad pathway(Liu et al., 2014; Suenaga et al., 2013), ERK signaling
574 pathway(Chiang et al., 2013), PDK1/Akt pathway(He et al., 2013), p38 MAPK/ATF-2
575 and TOR/p70 S6 kinase pathways(Yan et al., 2013). However, little is known about
576 pathways involved in preadipocytes differentiation of chicken. In our study, many
577 well-known pathways associated with different stages of differentiation such as ABC
578 transporters, jak-STAT, Wnt, Insulin, Fatty acid metabolism and Fatty acid
579 biosynthesis signaling pathways were found. Furthermore, we also identified many
580 pathways related to preadipocytes differentiation for the first time, including Oxidative
581 phosphorylation, Apoptosis, Propanoate metabolism and Galactose metabolism
582 signaling pathways. The enriched KEGG pathways associated with preadipocytes
583 differentiation in the mRNAs of stage-specific modules and potential lncRNAs targets
584 greatly expanded our knowledge on pathways involved in preadipocytes
585 differentiation.

586 To date, several previous studies have shown that PPARγ and C/EBPα(Yu et al.,
587 2014), FATP1(Qi et al., 2013) and Klf7(Zhang et al., 2013) regulate the differentiation
588 of preadipocytes in chicken. However, no study has been conducted on the roles of
589 lncRNAs in chicken preadipocytes differentiation. The molecular and cellular
590 mechanisms regulating chicken preadipocytes differentiation are still poorly
591 understood. Here, we identified a number of highly connected lncRNAs and mRNAs in

six stage-specific module. Those genes might play critical roles in each stage of preadipocytes differentiation in the chicken and were visualized by Cytoscape (Figure 7). The visualization of each module showed that the nodes number of lncRNAs were greater than that of mRNAs, demonstrating the regulation role of lncRNAs. Two lncRNAs (XLOC_068731 and XLOC_022661) and three protein-coding RNAs (*CHD6*, *LLGL1* and *NEURL1B*) were identified to be associated with day 2 of differentiation. *KLHL38* and XLOC_045161 were the highest connected mRNA and lncRNA, indicating their potential key roles in regulation of preadipocytes differentiation at day 6 of differentiation, while *ACTR6* and XLOC_070302, with the most connection, were found to be important factors in day 0 of differentiation. All the lncRNAs were novel and first identified. Those lncRNAs and mRNAs were validated by qRT-PCR and the results were in excellent agreement with the RNA-seq findings. It suggested that our findings in the present study were reliable. Besides, many well-known genes related to preadipocytes differentiation were found in the highly connected genes. For example, *IGFBP2* is a high connected gene in yellow module related to day 2 of differentiation and has inhibitory effect on preadipocyte differentiation in mice(Xi et al., 2013). It also inhibits both adipogenesis and lipogenesis in visceral(Yau et al., 2015). Similarly, *JUN* (AP-1) and *AP1B1* are highly connected genes in yellow and turquoise modules related to day 2 and day 0 of differentiation, respectively. Studies showed that *AP-1* controls adipocyte differentiation and survival by regulating *PPARγ* and hypoxia(Luther et al., 2014). *AP-1* also plays a role in regulating adipocyte differentiation and *FABP4* expression in 3T3-L1 cell(Kang et al., 2013). *AP1B1* regulates adipogenesis by mediating the sorting of sortilin in adipose tissue(Baltes et al., 2014).

Acknowledgments

This study was financially supported by the National Broiler Industrial and Technology System: nycytx-42-G1-05 and the Priority Academic Program Development of Jiangsu Higher Education Institutions. We have received funds for covering the costs to publish in open access.

Author Contributions

"Tao Zhang and Jinyu Wang conceived and designed the experiments; Tao Zhang and Xiangqian Zhang performed the experiments; Tao Zhang and Genxi Zhang analyzed the data; Kaizhou Xie, Kenpeng Han and Qian Xue contributed reagents/materials/analysis tools; Tao Zhang and Jinyu Wang wrote the paper."

Conflicts of Interest

The authors declare no conflict of interest.

Abbreviations

lncRNA	Long Non-coding RNA
DEGs	Differentially Expressed Genes
IGFBP2	Insulin like growth factor binding protein 2
JUN	Jun proto-oncogene
CDS	Coding sequence
UTR	Untranslated Regions
GO	Gene Ontology
KEGG	Kyoto Encyclopedia Of Genes And Genomes
WGCNA	Weighted Gene Co-expression Network Analysis
FDR	False Discovery Rate

GPR39	G protein-coupled receptor 39
AP-1	Transcription factor subunit
CHCHD4	Coiled-coil-helix-coiled-coil-helix domain containing 4
AP1B1	Adaptor related protein complex 1 beta 1 subunit
FABP4	Fatty acid binding protein 4
FBS	Fetal bovine serum
IBMX	3 isobutyl 1 methylxanthine

Reference

Alvarez-Dominguez, J. R., Bai, Z., Xu, D., Yuan, B., Lo, K. A., Yoon, M. J., Lim, Y. C., Knoll, M., Slavov, N., Chen, S., Chen, P., Lodish, H. F., and Sun, L. (2015). De Novo Reconstruction of Adipose Tissue Transcriptomes Reveals Long Non-coding RNA Regulators of Brown Adipocyte Development. *Cell Metab* **21**, 764-76.

Baltes, J., Larsen, J. V., Radhakrishnan, K., Geumann, C., Kratzke, M., Petersen, C. M., and Schu, P. (2014). sigma1B adaptin regulates adipogenesis by mediating the sorting of sortilin in adipose tissue. *J Cell Sci* **127**, 3477-87.

Banerjee, S. S., Feinberg, M. W., Watanabe, M., Gray, S., Haspel, R. L., Denkinger, D. J., Kawahara, R., Hauner, H., and Jain, M. K. (2003). The Kruppel-like factor KLF2 inhibits peroxisome proliferator-activated receptor-gamma expression and adipogenesis. *J Biol Chem* **278**, 2581-4.

Barabasi, A. L., and Oltvai, Z. N. (2004). Network biology: understanding the cell's functional organization. *Nat Rev Genet* **5**, 101-13.

Carlson, M. R., Zhang, B., Fang, Z., Mischel, P. S., Horvath, S., and Nelson, S. F. (2006). Gene connectivity, function, and sequence conservation: predictions from modular yeast co-expression networks. *BMC Genomics* **7**, 40.

Chen, J., Cui, X., Shi, C., Chen, L., Yang, L., Pang, L., Zhang, J., Guo, X., Wang, J., and Ji, C. (2015). Differential lncRNA expression profiles in brown and white adipose tissues. *Mol Genet Genomics* **290**, 699-707.

Chiang, P. Y., Shen, Y. F., Su, Y. L., Kao, C. H., Lin, N. Y., Hsu, P. H., Tsai, M. D., Wang, S. C., Chang, G. D., Lee, S. C., and Chang, C. J. (2013). Phosphorylation of mRNA decapping protein Dcp1a by the ERK signaling pathway during early differentiation of 3T3-L1 preadipocytes. *PLoS One* **8**, e61697.

de Jong, S., Boks, M. P., Fuller, T. F., Strengman, E., Janson, E., de Kovel, C. G., Ori, A. P., Vi, N., Mulder, F., Blom, J. D., Glenthoj, B., Schubart, C. D., Cahn, W., Kahn, R. S., Horvath, S., and Ophoff, R.

672 A. (2012). A gene co-expression network in whole blood of schizophrenia patients is
673 independent of antipsychotic-use and enriched for brain-expressed genes. *PLoS One* **7**,
674 e39498.
675 Demeure, O., Duclos, M. J., Bacciu, N., Le Mignon, G., Filangi, O., Pitel, F., Boland, A., Lagarrigue, S.,
676 Cogburn, L. A., Simon, J., Le Roy, P., and Le Bihan-Duval, E. (2013). Genome-wide interval
677 mapping using SNPs identifies new QTL for growth, body composition and several
678 physiological variables in an F2 intercross between fat and lean chicken lines. *Genet Sel Evol*
679 **45**, 36.
680 Ding, F., Li, Q. Q., Li, L., Gan, C., Yuan, X., Gou, H., He, H., Han, C. C., and Wang, J. W. (2015). Isolation,
681 culture and differentiation of duck (Anas platyrhynchos) preadipocytes. *Cytotechnology* **67**,
682 773-81.
683 Dong, J. Q., Zhang, H., Jiang, X. F., Wang, S. Z., Du, Z. Q., Wang, Z. P., Leng, L., Cao, Z. P., Li, Y. M., Luan,
684 P., and Li, H. (2015). Comparison of serum biochemical parameters between two broiler
685 chicken lines divergently selected for abdominal fat content. *J Anim Sci* **93**, 3278-86.
686 Dong, X., Tang, S., Zhang, W., Gao, W., and Chen, Y. (2016). GPR39 activates proliferation and
687 differentiation of porcine intramuscular preadipocytes through targeting the PI3K/AKT cell
688 signaling pathway. *J Recept Signal Transduct Res* **36**, 130-8.
689 Fuller, T. F., Ghazalpour, A., Aten, J. E., Drake, T. A., Lusis, A. J., and Horvath, S. (2007). Weighted gene
690 coexpression network analysis strategies applied to mouse weight. *Mamm Genome* **18**,
691 463-72.
692 Gupta, R. K., Arany, Z., Seale, P., Mepani, R. J., Ye, L., Conroe, H. M., Roby, Y. A., Kulaga, H., Reed, R. R.,
693 and Spiegelman, B. M. (2010). Transcriptional control of preadipocyte determination by
694 Zfp423. *Nature* **464**, 619-23.
695 Hartwell, L. H., Hopfield, J. J., Leibler, S., and Murray, A. W. (1999). From molecular to modular cell
696 biology. *Nature* **402**, C47-52.
697 He, Y., Li, Y., Zhang, S., Perry, B., Zhao, T., Wang, Y., and Sun, C. (2013). Radicicol, a heat shock protein
698 90 inhibitor, inhibits differentiation and adipogenesis in 3T3-L1 preadipocytes. *Biochem*
699 *Biophys Res Commun* **436**, 169-74.
700 Huang da, W., Sherman, B. T., and Lempicki, R. A. (2009). Systematic and integrative analysis of large
701 gene lists using DAVID bioinformatics resources. *Nat Protoc* **4**, 44-57.
702 Ji, B., Ernest, B., Gooding, J. R., Das, S., Saxton, A. M., Simon, J., Dupont, J., Metayer-Coustard, S.,
703 Campagna, S. R., and Voy, B. H. (2012). Transcriptomic and metabolomic profiling of chicken
704 adipose tissue in response to insulin neutralization and fasting. *BMC Genomics* **13**, 441.
705 Jiang, Z., Sun, J., Dong, H., Luo, O., Zheng, X., Obergfell, C., Tang, Y., Bi, J., O'Neill, R., Ruan, Y., Chen, J.,
706 and Tian, X. C. (2014). Transcriptional profiles of bovine in vivo pre-implantation
707 development. *BMC Genomics* **15**, 756.
708 Kaczynski, J., Cook, T., and Urrutia, R. (2003). Sp1- and Kruppel-like transcription factors. *Genome Biol*
709 **4**, 206.
710 Kang, M., Yan, L. M., Li, Y. M., Zhang, W. Y., Wang, H., Tang, A. Z., and Ou, H. S. (2013). Inhibitory
711 effect of microRNA-24 on fatty acid-binding protein expression on 3T3-L1 adipocyte
712 differentiation. *Genet Mol Res* **12**, 5267-77.

Kershaw, E. E., and Flier, J. S. (2004). Adipose tissue as an endocrine organ. *J Clin Endocrinol Metab* **89**, 2548-56.

Langfelder, P., and Horvath, S. (2008). WGCNA: an R package for weighted correlation network analysis. *BMC Bioinformatics* **9**, 559.

Leclercq, B. (1984). Adipose tissue metabolism and its control in birds. *Poult Sci* **63**, 2044-54.

Liu, Y., Liu, Y., Zhang, R., Wang, X., Huang, F., Yan, Z., Nie, M., Huang, J., Wang, Y., Wang, Y., Chen, L., Yin, L., He, B., and Deng, Z. (2014). All-trans retinoic acid modulates bone morphogenic protein 9-induced osteogenesis and adipogenesis of preadipocytes through BMP/Smad and Wnt/beta-catenin signaling pathways. *Int J Biochem Cell Biol* **47**, 47-56.

Lu, H., Li, X., Mu, P., Qian, B., Jiang, W., and Zeng, L. (2016). Dickkopf-1 promotes the differentiation and adipocytokines secretion via canonical Wnt signaling pathway in primary cultured human preadipocytes. *Obes Res Clin Pract* **10**, 454-64.

Luan, A., Paik, K. J., Li, J., Zielins, E. R., Atashroo, D. A., Spencley, A., Momeni, A., Longaker, M. T., Wang, K. C., and Wan, D. C. (2015). RNA Sequencing for Identification of Differentially Expressed Noncoding Transcripts during Adipogenic Differentiation of Adipose-Derived Stromal Cells. *Plast Reconstr Surg* **136**, 752-63.

Luther, J., Ubieta, K., Hannemann, N., Jimenez, M., Garcia, M., Zech, C., Schett, G., Wagner, E. F., and Bozec, A. (2014). Fra-2/AP-1 controls adipocyte differentiation and survival by regulating PPARgamma and hypoxia. *Cell Death Differ* **21**, 655-64.

MacDougald, O. A., and Lane, M. D. (1995). Transcriptional regulation of gene expression during adipocyte differentiation. *Annu Rev Biochem* **64**, 345-73.

Mai, Y., Zhang, Z., Yang, H., Dong, P., Chu, G., Yang, G., and Sun, S. (2014). BMP and activin membrane-bound inhibitor (BAMBI) inhibits the adipogenesis of porcine preadipocytes through Wnt/beta-catenin signaling pathway. *Biochem Cell Biol* **92**, 172-82.

Matsubara, Y., Aoki, M., Endo, T., and Sato, K. (2013). Characterization of the expression profiles of adipogenesis-related factors, ZNF423, KLFs and FGF10, during preadipocyte differentiation and abdominal adipose tissue development in chickens. *Comp Biochem Physiol B Biochem Mol Biol* **165**, 189-95.

Matsubara, Y., Sato, K., Ishii, H., and Akiba, Y. (2005). Changes in mRNA expression of regulatory factors involved in adipocyte differentiation during fatty acid induced adipogenesis in chicken. *Comp Biochem Physiol A Mol Integr Physiol* **141**, 108-15.

Mori, T., Sakaue, H., Iguchi, H., Gomi, H., Okada, Y., Takashima, Y., Nakamura, K., Nakamura, T., Yamauchi, T., Kubota, N., Kadowaki, T., Matsuki, Y., Ogawa, W., Hiramatsu, R., and Kasuga, M. (2005). Role of Kruppel-like factor 15 (KLF15) in transcriptional regulation of adipogenesis. *J Biol Chem* **280**, 12867-75.

Morrison, R. F., and Farmer, S. R. (2000). Hormonal signaling and transcriptional control of adipocyte differentiation. *J Nutr* **130**, 3116s-3121s.

Park, J. G., Lee, D. H., Moon, Y. S., and Kim, K. H. (2014). Reversine increases the plasticity of lineage-committed preadipocytes to osteogenesis by inhibiting adipogenesis through induction of TGF-beta pathway in vitro. *Biochem Biophys Res Commun* **446**, 30-6.

Qi, R., Feng, M., Tan, X., Gan, L., Yan, G., and Sun, C. (2013). FATP1 silence inhibits the differentiation and induces the apoptosis in chicken preadipocytes. *Mol Biol Rep* **40**, 2907-14.

Quinlan, A. R., and Hall, I. M. (2010). BEDTools: a flexible suite of utilities for comparing genomic features. *Bioinformatics* **26**, 841-2.

Regassa, A., and Kim, W. K. (2015). Transcriptome analysis of hen preadipocytes treated with an adipogenic cocktail (DMIOA) with or without 20(S)-hydroxylcholesterol. *BMC Genomics* **16**, 91.

Ren, H., Wang, G., Chen, L., Jiang, J., Liu, L., Li, N., Zhao, J., Sun, X., and Zhou, P. (2016). Genome-wide analysis of long non-coding RNAs at early stage of skin pigmentation in goats (Capra hircus). *BMC Genomics* **17**, 67.

Resnyk, C. W., Carre, W., Wang, X., Porter, T. E., Simon, J., Le Bihan-Duval, E., Duclos, M. J., Aggrey, S. E., and Cogburn, L. A. (2013). Transcriptional analysis of abdominal fat in genetically fat and lean chickens reveals adipokines, lipogenic genes and a link between hemostasis and leanness. *BMC Genomics* **14**, 557.

Resnyk, C. W., Chen, C., Huang, H., Wu, C. H., Simon, J., Le Bihan-Duval, E., Duclos, M. J., and Cogburn, L. A. (2015). RNA-Seq Analysis of Abdominal Fat in Genetically Fat and Lean Chickens Highlights a Divergence in Expression of Genes Controlling Adiposity, Hemostasis, and Lipid Metabolism. *PLoS One* **10**, e0139549.

Sakaue, H., Konishi, M., Ogawa, W., Asaki, T., Mori, T., Yamasaki, M., Takata, M., Ueno, H., Kato, S., Kasuga, M., and Itoh, N. (2002). Requirement of fibroblast growth factor 10 in development of white adipose tissue. *Genes Dev* **16**, 908-12.

Shang, Z., Guo, L., Wang, N., Shi, H., Wang, Y., and Li, H. (2014). Oleate promotes differentiation of chicken primary preadipocytes in vitro. *Bioscience Reports* **34**, 51-57.

Suenaga, M., Kurosawa, N., Asano, H., Kanamori, Y., Umemoto, T., Yoshida, H., Murakami, M., Kawachi, H., Matsui, T., and Funaba, M. (2013). Bmp4 expressed in preadipocytes is required for the onset of adipocyte differentiation. *Cytokine* **64**, 138-45.

Trapnell, C., Hendrickson, D. G., Sauvageau, M., Goff, L., Rinn, J. L., and Pachter, L. (2013). Differential analysis of gene regulation at transcript resolution with RNA-seq. *Nat Biotechnol* **31**, 46-53.

Trapnell, C., Roberts, A., Goff, L., Pertea, G., Kim, D., Kelley, D. R., Pimentel, H., Salzberg, S. L., Rinn, J. L., and Pachter, L. (2012). Differential gene and transcript expression analysis of RNA-seq experiments with TopHat and Cufflinks. *Nat Protoc* **7**, 562-78.

Trapnell, C., Williams, B. A., Pertea, G., Mortazavi, A., Kwan, G., van Baren, M. J., Salzberg, S. L., Wold, B. J., and Pachter, L. (2010). Transcript assembly and quantification by RNA-Seq reveals unannotated transcripts and isoform switching during cell differentiation. *Nat Biotechnol* **28**, 511-5.

Tung, Y. C., Li, S., Huang, Q., Hung, W. L., Ho, C. T., Wei, G. J., and Pan, M. H. (2016). 5-Demethylnobiletin and 5-Acetoxy-6,7,8,3',4'-pentamethoxyflavone Suppress Lipid Accumulation by Activating the LKB1-AMPK Pathway in 3T3-L1 Preadipocytes and High Fat Diet-Fed C57BL/6 Mice. *J Agric Food Chem* **64**, 3196-205.

Wang, W., Du, Z. Q., Cheng, B., Wang, Y., Yao, J., Li, Y., Cao, Z., Luan, P., Wang, N., and Li, H. (2015). Expression profiling of preadipocyte microRNAs by deep sequencing on chicken lines divergently selected for abdominal fatness. *PLoS One* **10**, e0117843.

795 Wang, Y., Xue, S., Liu, X., Liu, H., Hu, T., Qiu, X., Zhang, J., and Lei, M. (2016). Analyses of Long
796 Non-Coding RNA and mRNA profiling using RNA sequencing during the pre-implantation
797 phases in pig endometrium. *Sci Rep* **6**, 20238.
798 Xi, G., Solum, M. A., Wai, C., Maile, L. A., Rosen, C. J., and Clemmons, D. R. (2013). The heparin-binding
799 domains of IGFBP-2 mediate its inhibitory effect on preadipocyte differentiation and fat
800 development in male mice. *Endocrinology* **154**, 4146-57.
801 Yamasaki, M., Emoto, H., Konishi, M., Mikami, T., Ohuchi, H., Nakao, K., and Itoh, N. (1999). FGF-10 is
802 a growth factor for preadipocytes in white adipose tissue. *Biochem Biophys Res Commun* **258**,
803 109-12.
804 Yan, J., Gan, L., Chen, D., and Sun, C. (2013). Adiponectin impairs chicken preadipocytes
805 differentiation through p38 MAPK/ATF-2 and TOR/p70 S6 kinase pathways. *PLoS One* **8**,
806 e77716.
807 Yau, S. W., Russo, V. C., Clarke, I. J., Dunshea, F. R., Werther, G. A., and Sabin, M. A. (2015). IGFBP-2
808 inhibits adipogenesis and lipogenesis in human visceral, but not subcutaneous, adipocytes.
809 *Int J Obes (Lond)* **39**, 770-81.
810 Ye, M., Wang, Z., Wang, Y., and Wu, R. (2015). A multi-Poisson dynamic mixture model to cluster
811 developmental patterns of gene expression by RNA-seq. *Brief Bioinform* **16**, 205-15.
812 You, L. H., Zhu, L. J., Yang, L., Shi, C. M., Pang, L. X., Zhang, J., Cui, X. W., Ji, C. B., and Guo, X. R. (2015).
813 Transcriptome analysis reveals the potential contribution of long noncoding RNAs to brown
814 adipocyte differentiation. *Mol Genet Genomics* **290**, 1659-71.
815 Yu, X., Liu, R., Zhao, G., Zheng, M., Chen, J., and Wen, J. (2014). Folate supplementation modifies
816 CCAAT/enhancer-binding protein alpha methylation to mediate differentiation of
817 preadipocytes in chickens. *Poult Sci* **93**, 2596-603.
818 Zhang, B., and Horvath, S. (2005). A general framework for weighted gene co-expression network
819 analysis. *Stat Appl Genet Mol Biol* **4**, Article17.
820 Zhang, Z., Wang, H., Sun, Y., Li, H., and Wang, N. (2013). Klf7 modulates the differentiation and
821 proliferation of chicken preadipocyte. *Acta Biochim Biophys Sin (Shanghai)* **45**, 280-8.
822 Zhang, Z. W., Rong, E. G., Shi, M. X., Wu, C. Y., Sun, B., Wang, Y. X., Wang, N., and Li, H. (2014a).
823 Expression and functional analysis of Kruppel-like factor 2 in chicken adipose tissue. *J Anim*
824 *Sci* **92**, 4797-805.
825 Zhang, Z. W., Wu, C. Y., Li, H., and Wang, N. (2014b). Expression and functional analyses of
826 Kruppel-like factor 3 in chicken adipose tissue. *Biosci Biotechnol Biochem* **78**, 614-23.
827 Zhang, Z. Y., Mai, Y., Yang, H., Dong, P. Y., Zheng, X. L., and Yang, G. S. (2014c). CTSB promotes porcine
828 preadipocytes differentiation by degrading fibronectin and attenuating the Wnt/beta-catenin
829 signaling pathway. *Mol Cell Biochem* **395**, 53-64.
830 Zhao, X. Y., and Lin, J. D. (2015). Long Noncoding RNAs: A New Regulatory Code in Metabolic Control.
831 *Trends Biochem Sci* **40**, 586-96.
832 Zhuo, Z., Lamont, S. J., Lee, W. R., and Abasht, B. (2015). RNA-Seq Analysis of Abdominal Fat Reveals
833 Differences between Modern Commercial Broiler Chickens with High and Low Feed
834 Efficiencies. *PLoS One* **10**, e0135810.

835